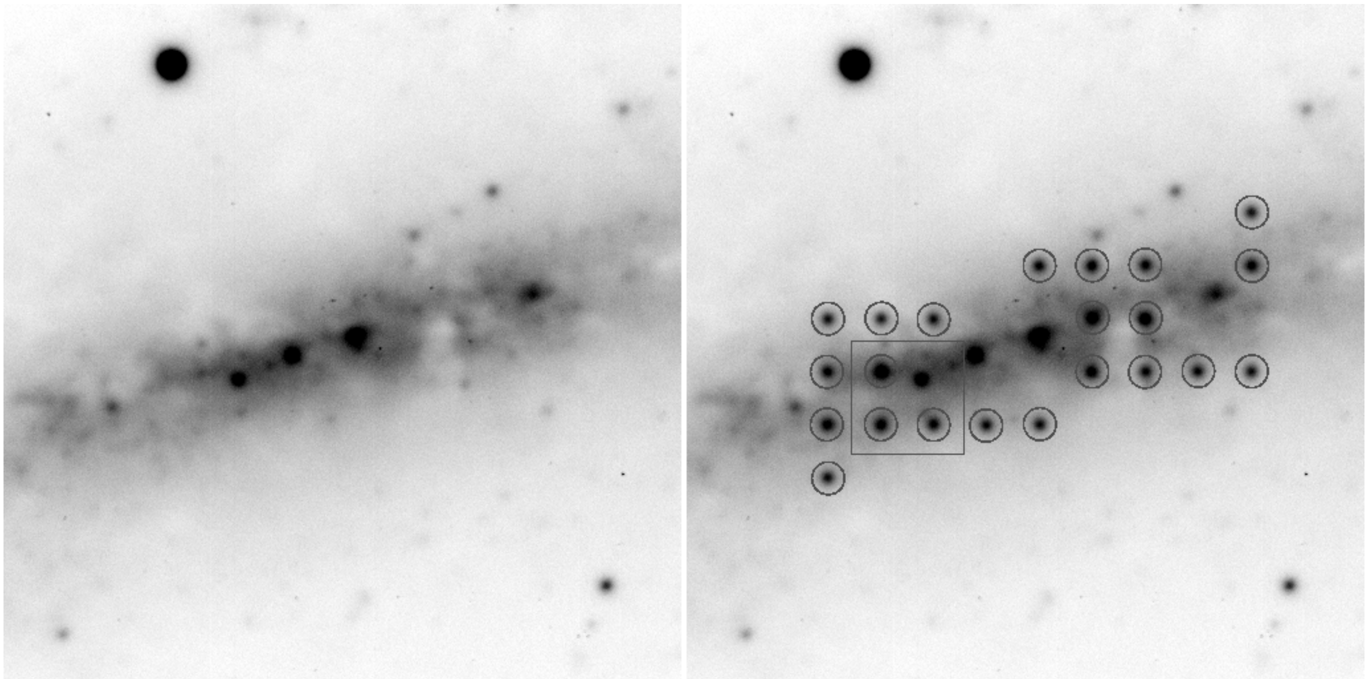

Fig. 2. a) Left: The galaxy NGC 672. b) Right: The galaxy NGC 672 with simulated stars added. The simulated stars are marked with dark rings. The small area inside the dark frame is shown magnified in Figure 3.

Fig. 3. a) Left: The small area of NGC 672 inside the dark frame in Figure 2 magnified 4 times. The area contains 3 simulated and 1 observed star. b) Center: The resulting background image when the stars in (a) are measured and subtracted using POLYFIT. A fitting radius of $1.5 \cdot \mathrm{FWHM}$ of the stars and a polynomial degree of 2 were used. Only some faint residuals can be seen. c) Right: The same area as in (a) and (b) without simulated stars for comparison.

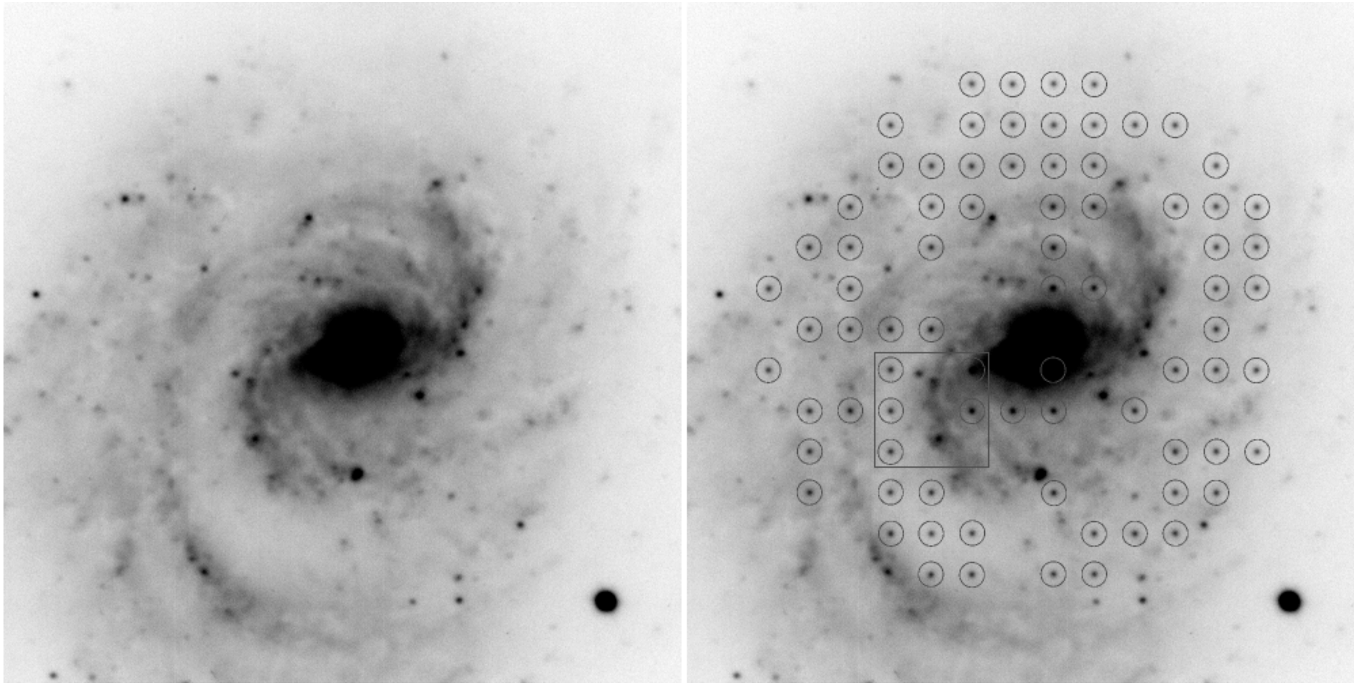

Fig. 4. a) Left: The galaxy NGC 1637. b) Right: The galaxy NGC 1637 with simulated stars added. The simulated stars are marked with dark rings. The small area inside the dark frame is shown magnified in Figure 5.

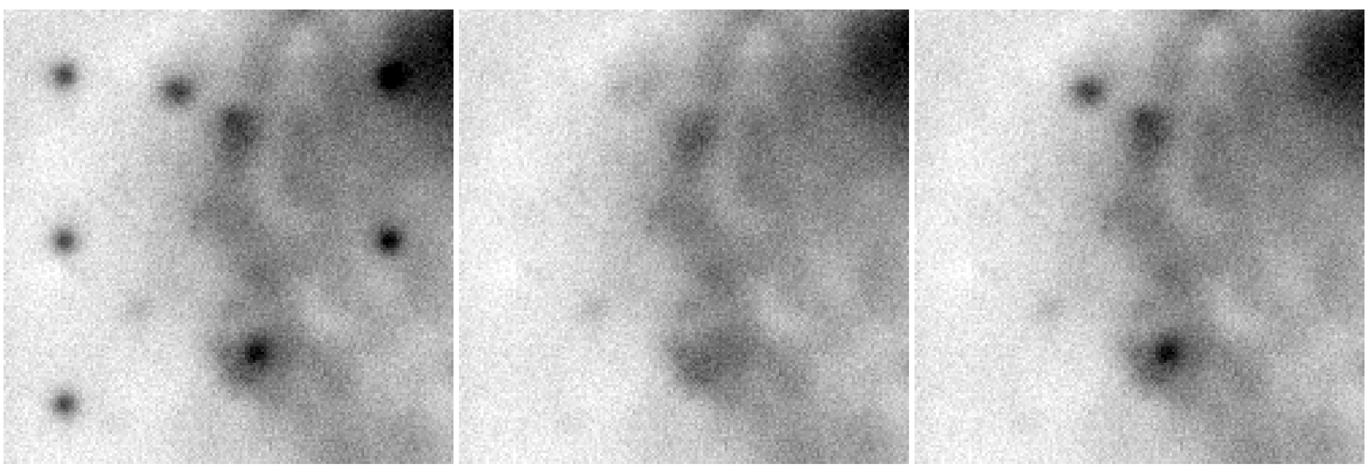

Fig. 5. a) Left: The small area of NGC 1637 inside the dark frame in Figure 4 magnified 4 times. The area contains 5 simulated and 3 observed stars. b) Center: The resulting background image when the stars in (a) are measured and subtracted using POLYFIT. A fitting radius of $1.5 \cdot \mathrm{FWHM}$ of the stars and a polynomial degree of 2 were used. Only some faint residuals can be seen. c) Right: The same area as in (a) and (b) without simulated stars for comparison.

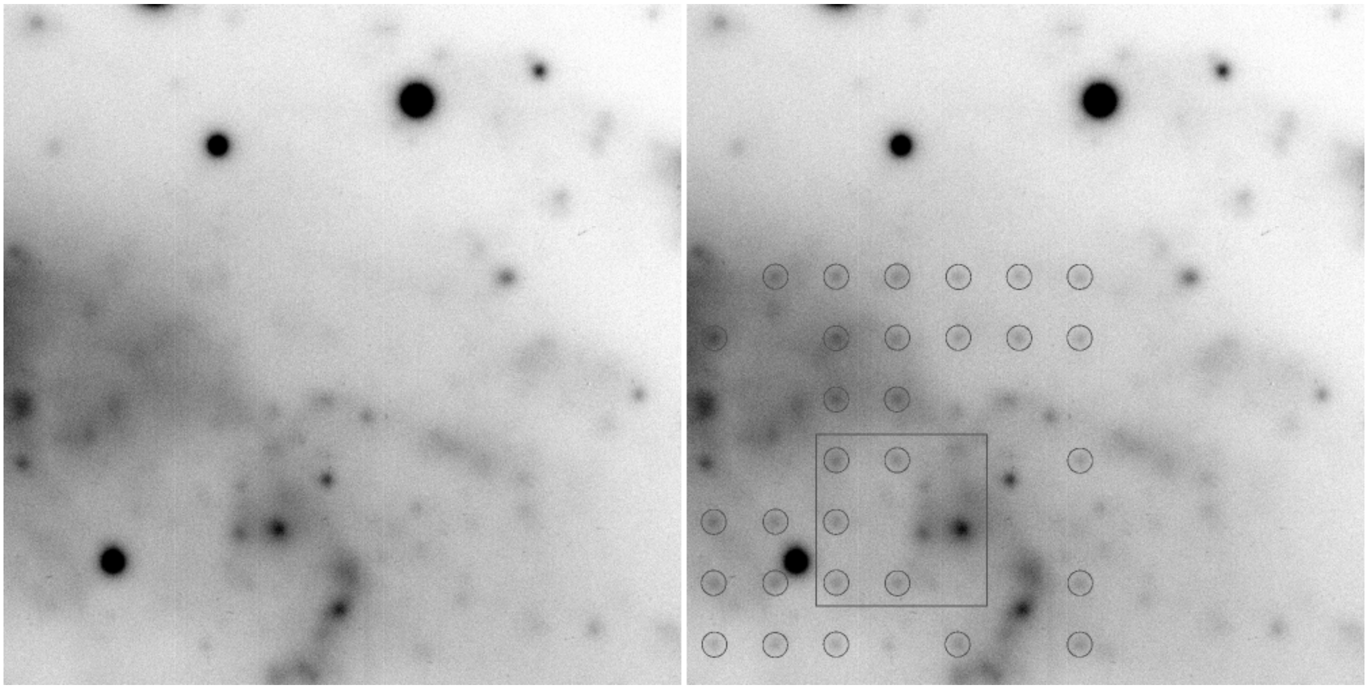

Fig. 6. a) Left: The galaxy NGC 925. b) Right: The galaxy NGC 925 with simulated stars added. The simulated stars are marked with dark rings. They look faint due to the large FWHM of the PSF. The small area inside the dark frame is shown magnified in Figure 7.

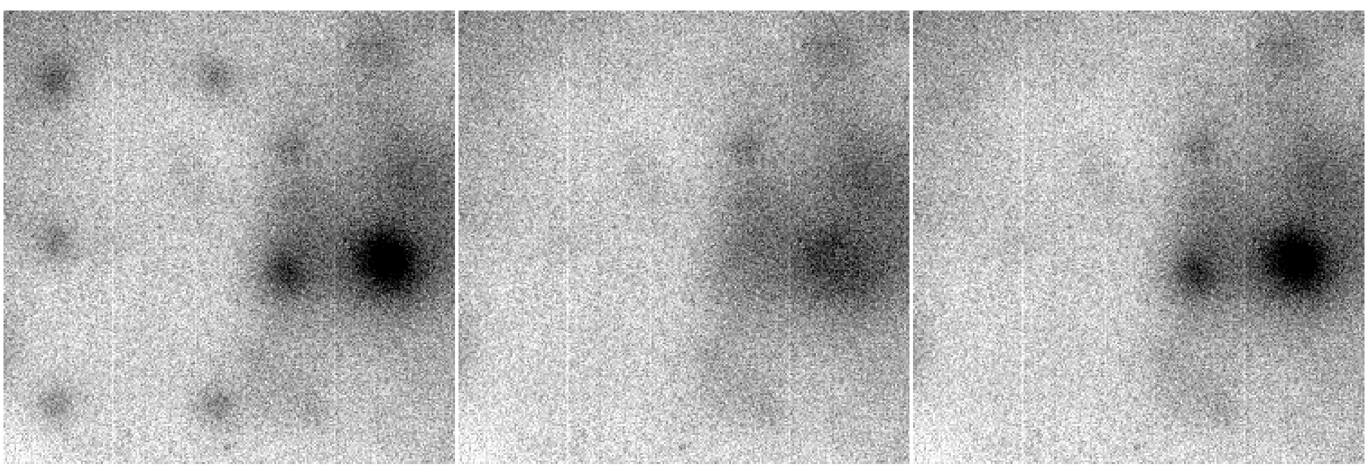

Fig. 7. a) Left: The small area of NGC 925 inside the dark frame in Figure 6 magnified 2.7 times. The area contains 5 simulated and 2 observed stars. b) Center: The resulting background image when the stars in (a) are measured and subtracted using POLYFIT. A fitting radius of $1.5 \cdot \mathrm{FWHM}$ of the stars and a polynomial degree of 2 were used. Only some faint residuals can be seen. c) Right: The same area as in (a) and (b) without simulated stars for comparison.

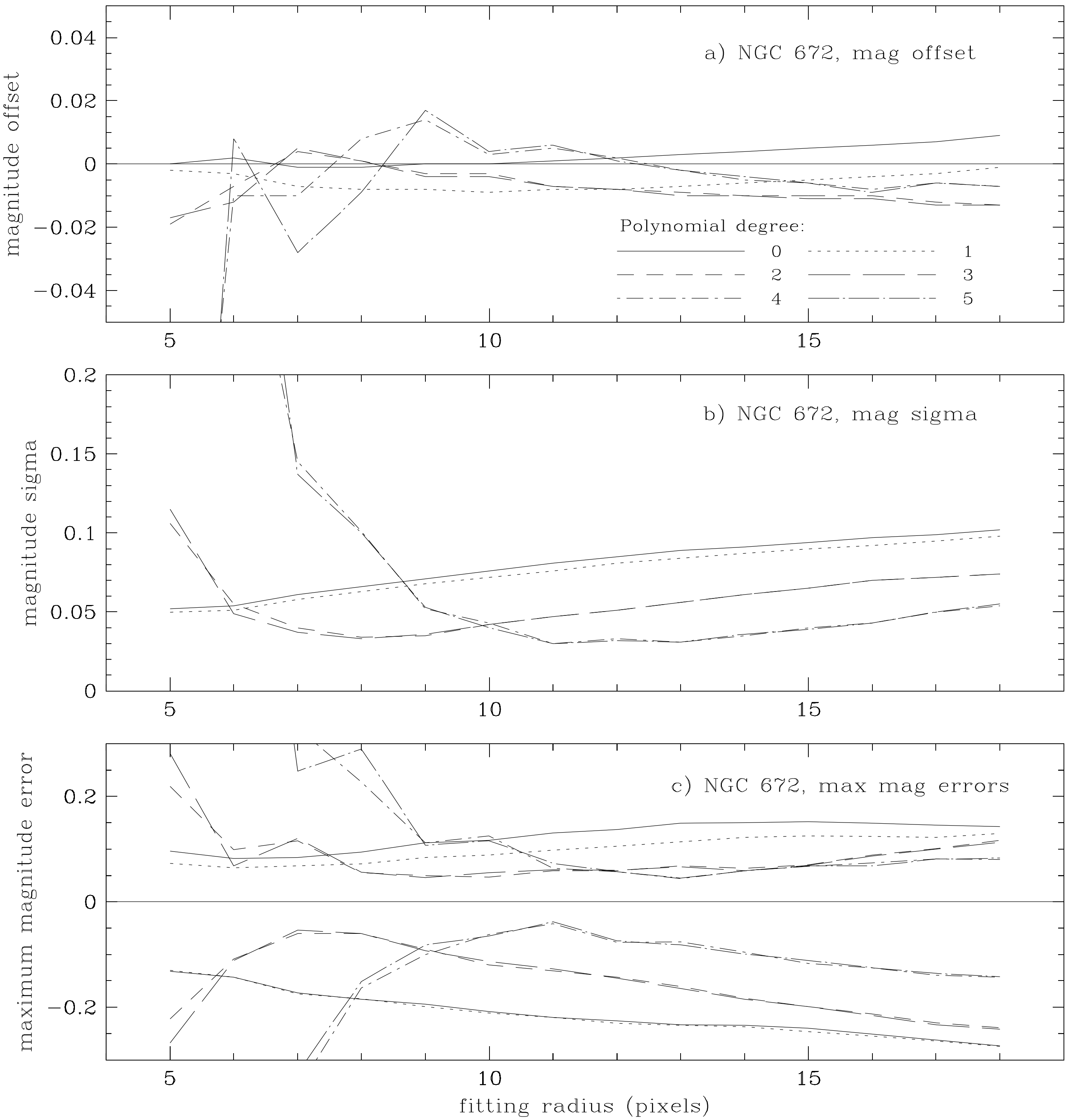

Fig. 8. Photometric results with POLYFIT from simulated stars added to the galaxy NGC 672. a) Upper panel: The average magnitude offsets as function of fitting radius for different degrees the background polynomials are shown. The different line types correspond to different degree of the background polynomial as shown with the numbers by the short lines. b) Middle panel: The standard deviation (σ) in magnitude as function of the fitting radius for different degrees of the background polynomials are shown. c) Lower panel: Maximum magnitude errors (both positive and negative) as function of fitting radius for different degrees of the background polynomials are shown.

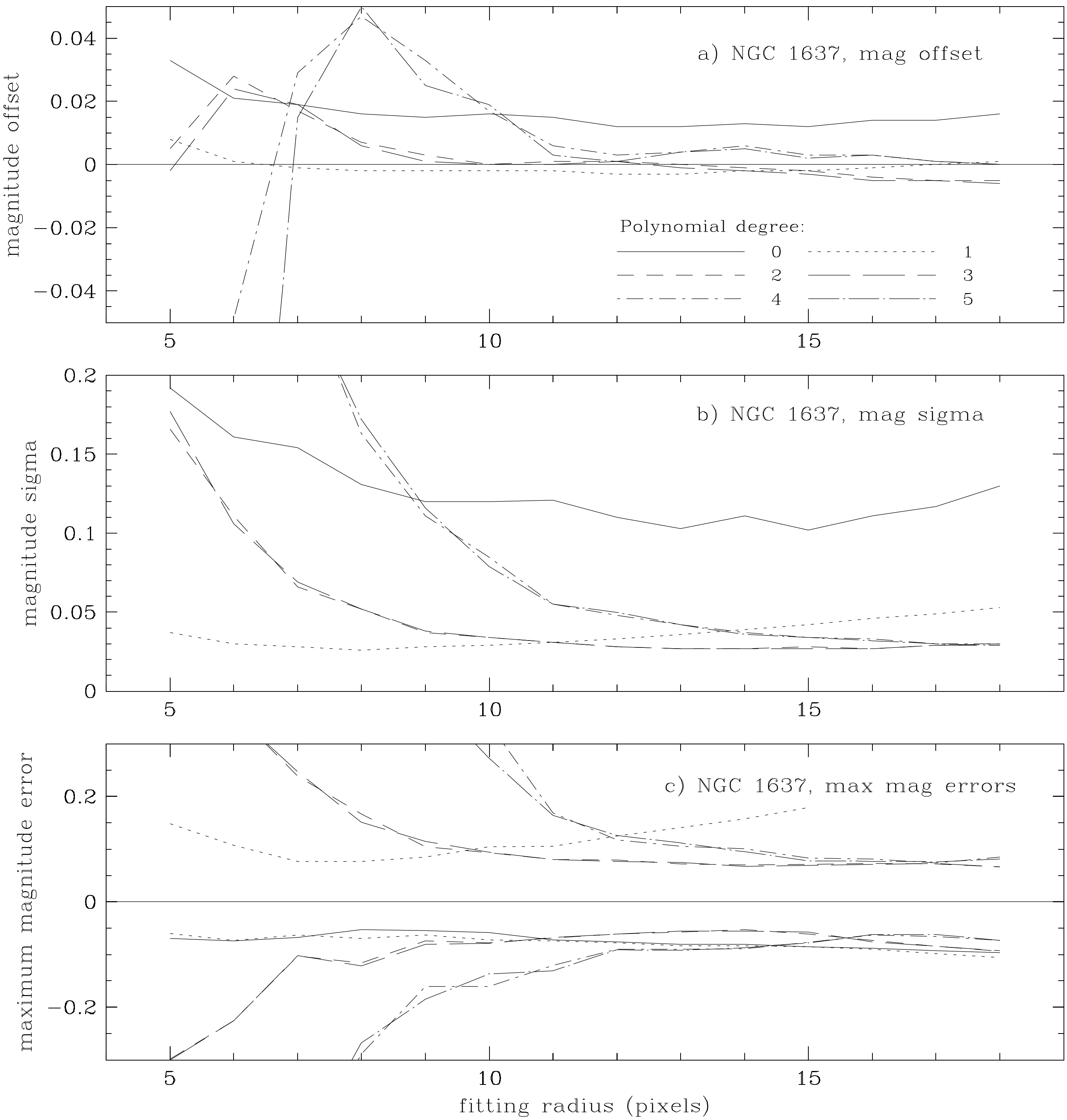

Fig. 9. Same as Figure 8 but for the galaxy NGC 1637. Polynomial degree 0 show large deviations for σ and the positive maximum error because one or a few stars have been erroneously measured.

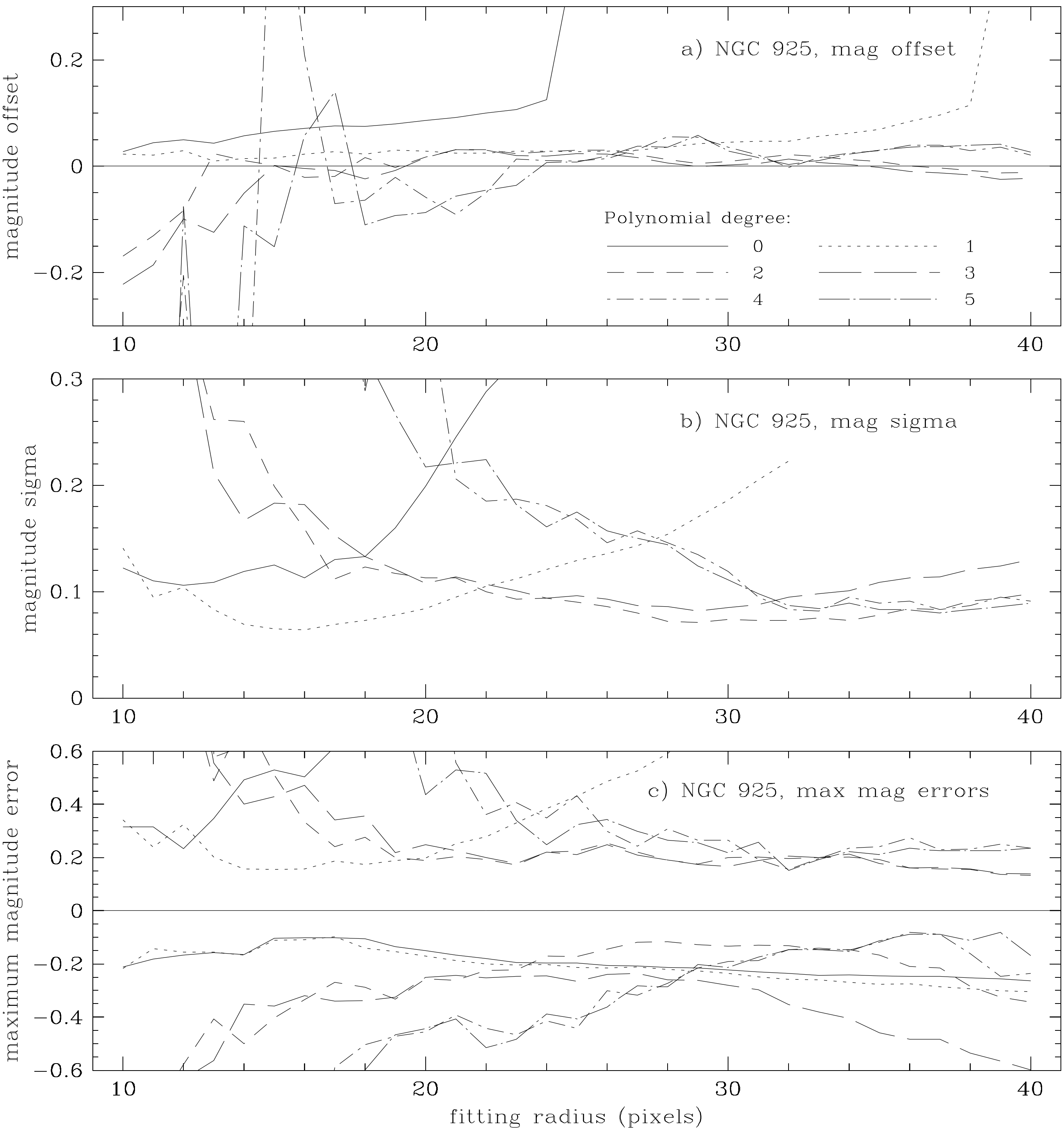

Fig. 10. Same as Figure 8 but for the galaxy NGC 925. Polynomial degree 0 and 1 show large deviations for σ and the positive maximum error because one or a few stars have been erroneously measured.

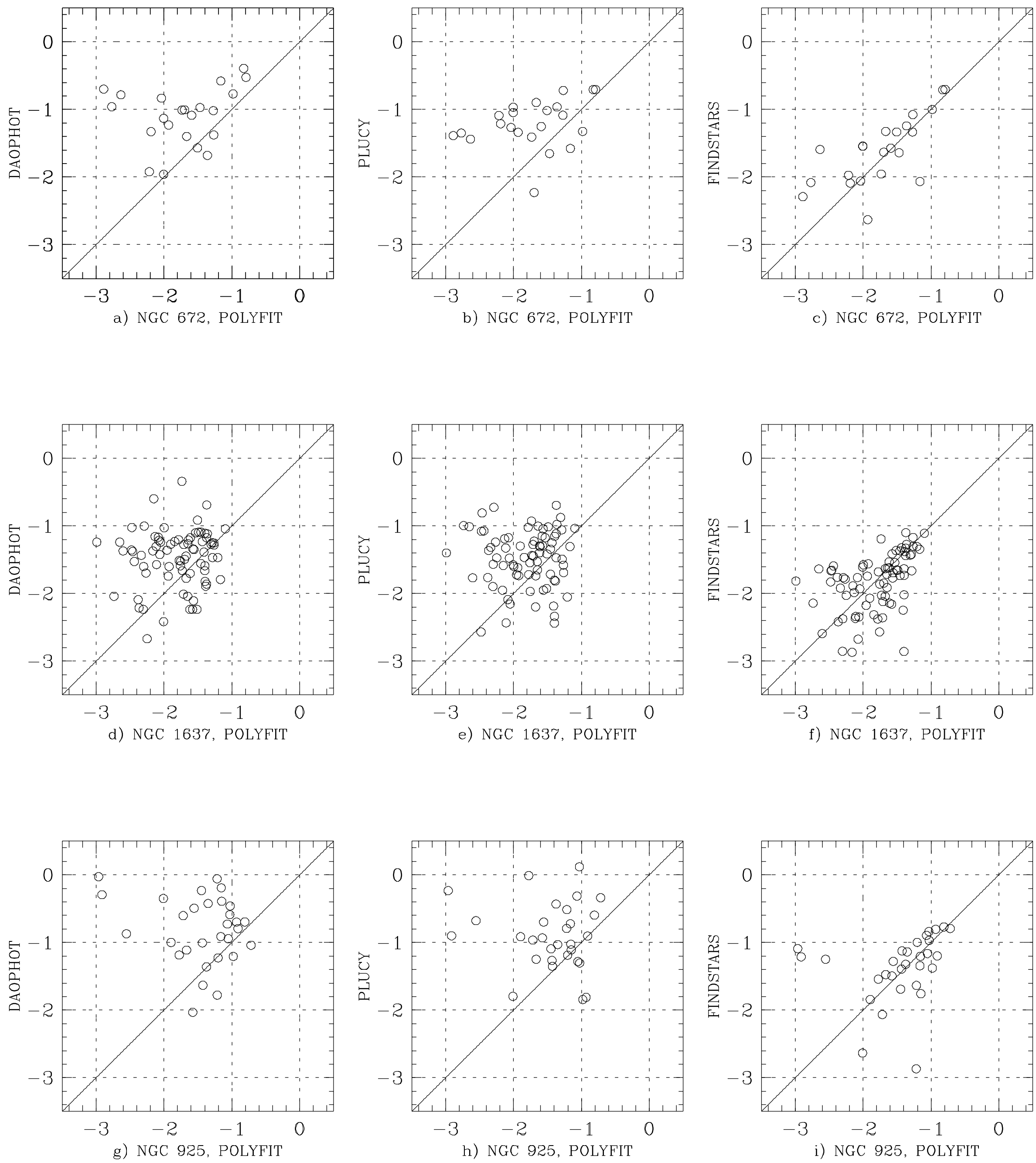

Fig. 11. Logarithmic magnitude error diagrams for simulated stars added to images of the galaxies NGC 672, NGC 1637 and NGC 925 for comparison between POLYFIT–DAOPHOT, POLYFIT–PLUCY and POLYFIT–FINDSTARS. A fitting radius of $1.5 \cdot$ FWHM of the stellar image and polynomial degree of 2 have been used for POLYFIT. Stars with errors above the diagonal line are better for POLYFIT. For most stars POLYFIT is the better program.

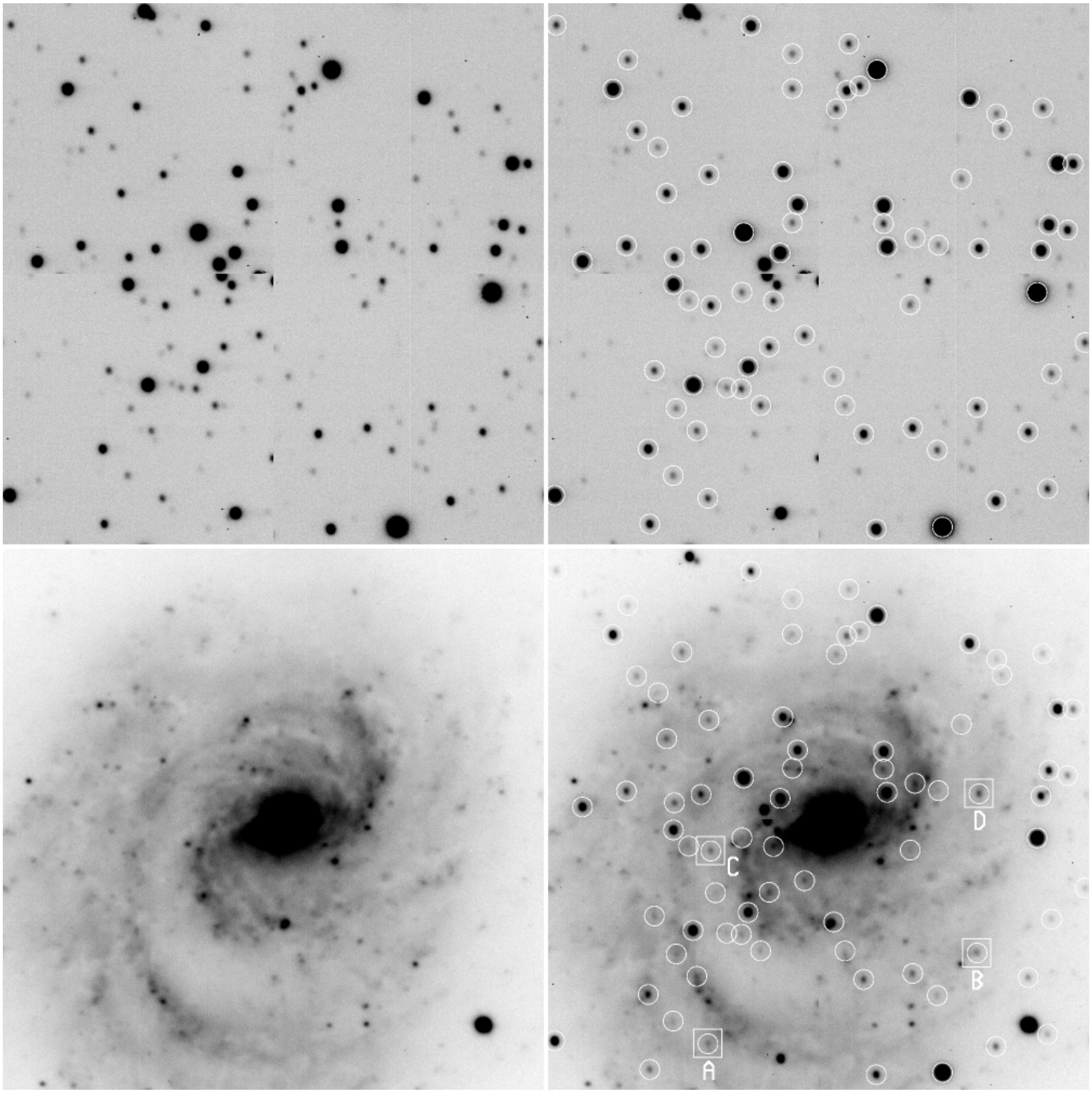

Fig. 12. a) Upper left: The open cluster NGC 7790. The four quadrants of the image are diagonally shifted to get more stars in the center of the image. b) Upper right: The same image as in (a). The 77 stars included in the test are marked with white rings. c) Lower left: The galaxy NGC 1637. d) Lower right: The galaxy NGC 1637 with the open cluster NGC 7790 image added. The 77 stars included in the test are marked with white rings. The stellar images inside the white frames A–D are shown in magnified scale in Figures 15–18.

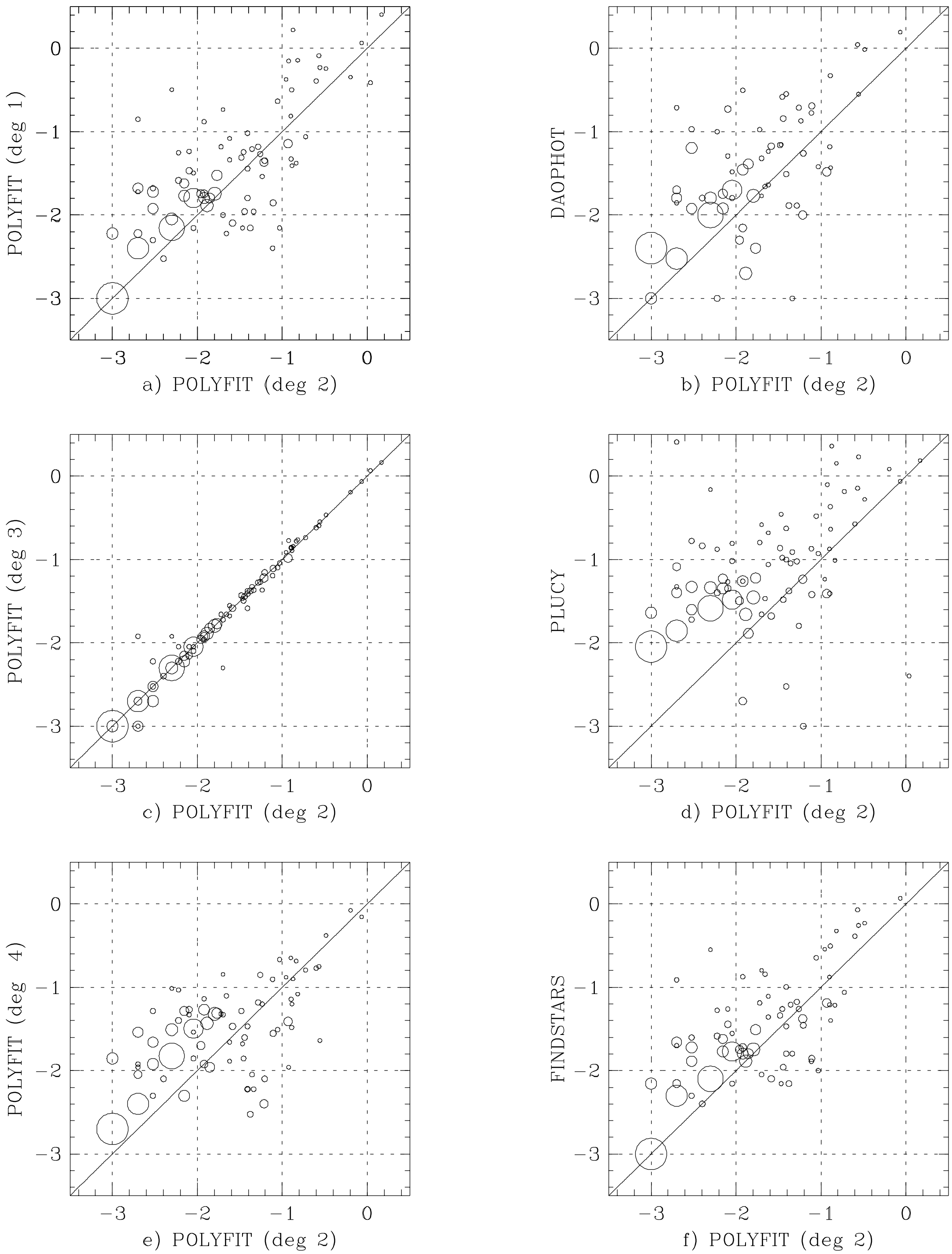

Fig. 13. Logarithmic magnitude error diagrams for measured stars in the combined open cluster (NGC 7790) plus galaxy (NGC 1637) image. The areas of the circles are proportional to the intensities of the stars. A fitting radius of $1.5 \cdot \mathrm{FWHM}$ of the stellar image and polynomial degree of 2 gives the best result for POLYFIT. This result is compared with results from POLYFIT degree 1, 3 and 4 (diagrams a, c and e) and results from DAOPHOT, PLUCY and FINDSTARS (diagrams b, d and f). Not all 77 stars were found with the automatic programs DAOPHOT (61 stars) and FINDSTARS (70 stars). The results for POLYFIT with polynomial degree 2 and 3 are equally good for most stars. This is due to the pair effect described in Section 6.1.1.

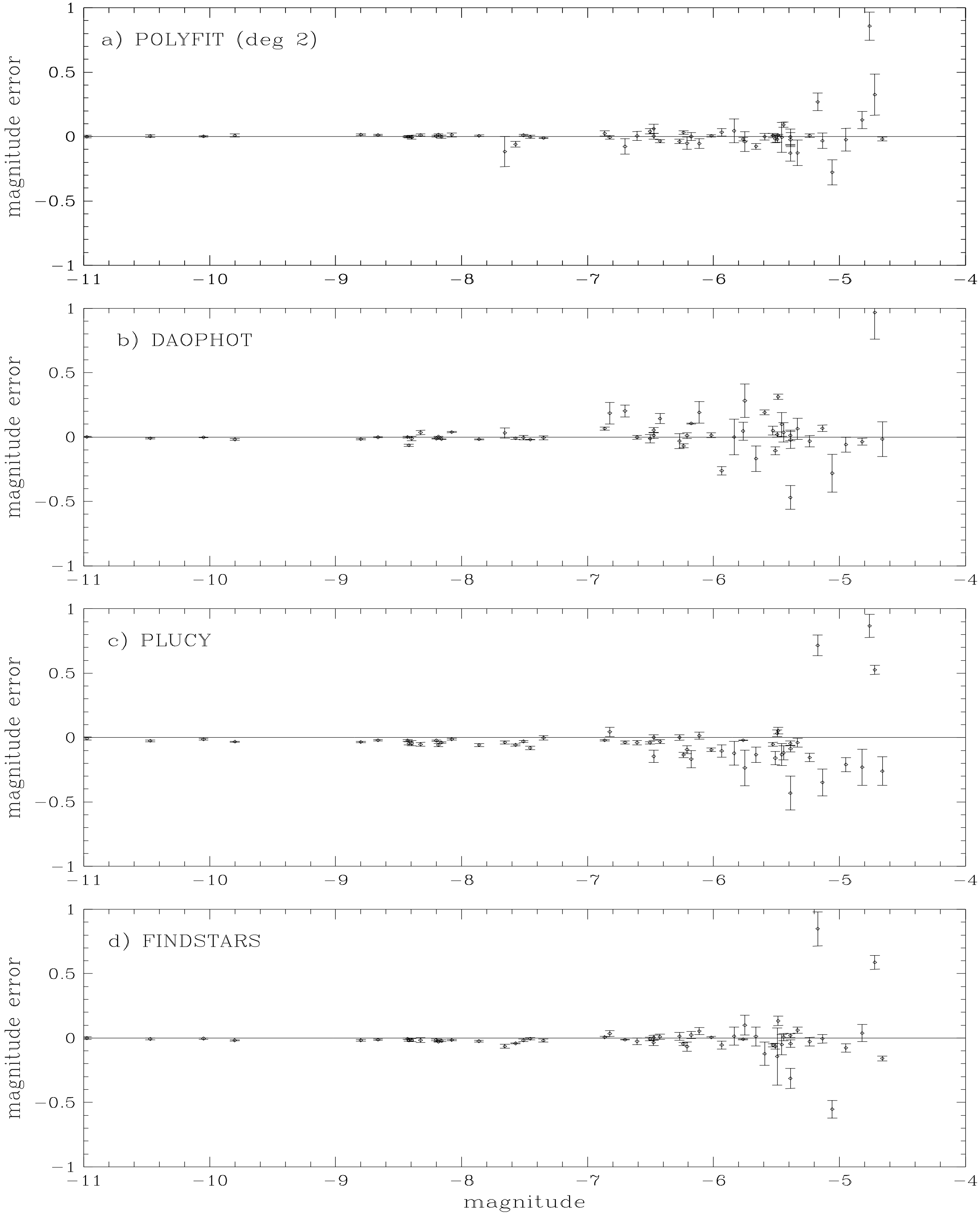

Fig. 14. Magnitude offsets and standard deviations for the three measurements of each star in the combined open cluster (NGC 7790) plus galaxy (NGC 1637) images. Results from 59 stars (of total 77) that are found also with both the automatic programs DAOPHOT and FINDSTARS are presented. POLYFIT was the best program for most stars. A fitting radius of $1.5 \cdot \mathrm{FWHM}$ of the stellar image and polynomial degree of 2 was used for this program. Magnitude -5 corresponds to an intensity of approximately 10000 ADU. From above: a) POLYFIT (degree 2). b) DAOPHOT. c) PLUCY. d) FINDSTARS.

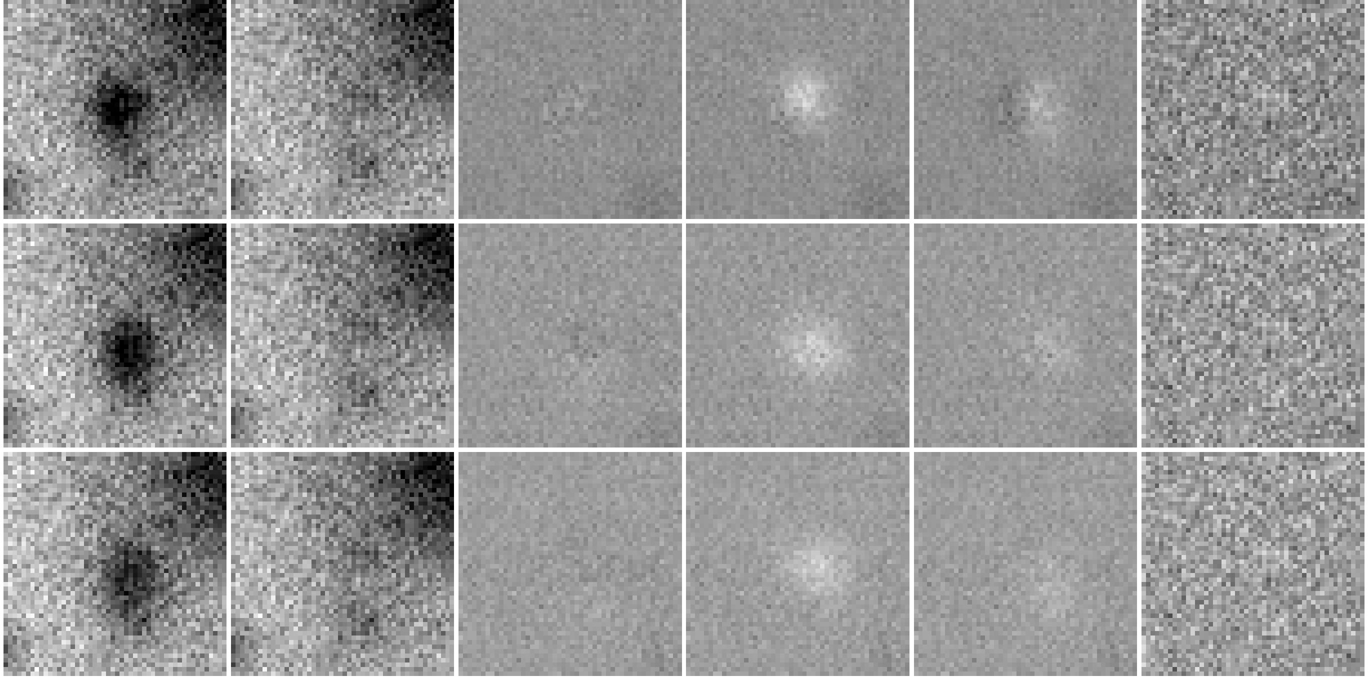

Fig. 15. Frame A in Figure 12 d. All the three different open cluster plus galaxy images are shown (row 1–3). In this figure residual image means the galaxy plus the open cluster image minus the measured star and the galaxy image. Counted from the left, the first column shows the small open cluster plus galaxy frame (including the measured star). The second column shows the true galaxy background without the open cluster star. The third column represents the residual image obtained by POLYFIT (degree 2). The fourth column represents the residual images obtained by DAOPHOT. The fifth column shows the residual images obtained with FINDSTARS. Finally the sixth column shows the residual images obtained by PLUCY. These residual images look noisy due to the fact that the program smoothes the background image using a Gaussian filter.

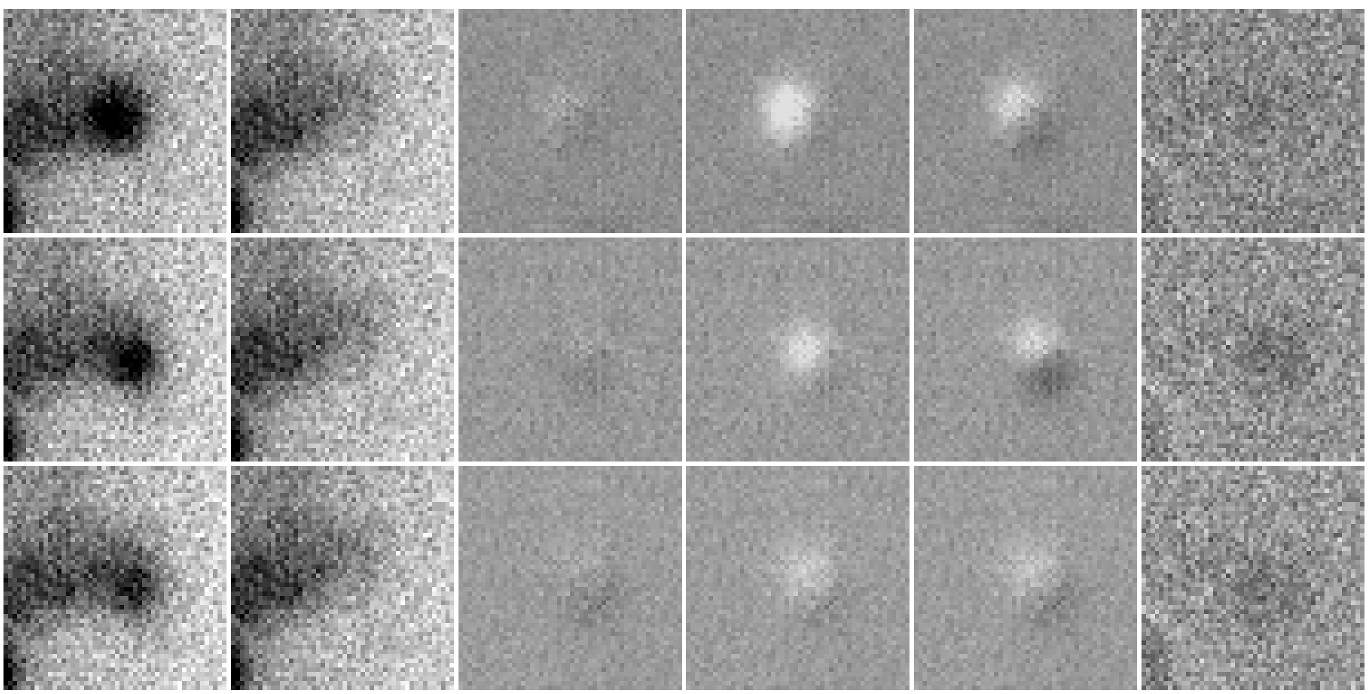

Fig. 16. Same as Figure 15 but for frame B in Figure 12 d.

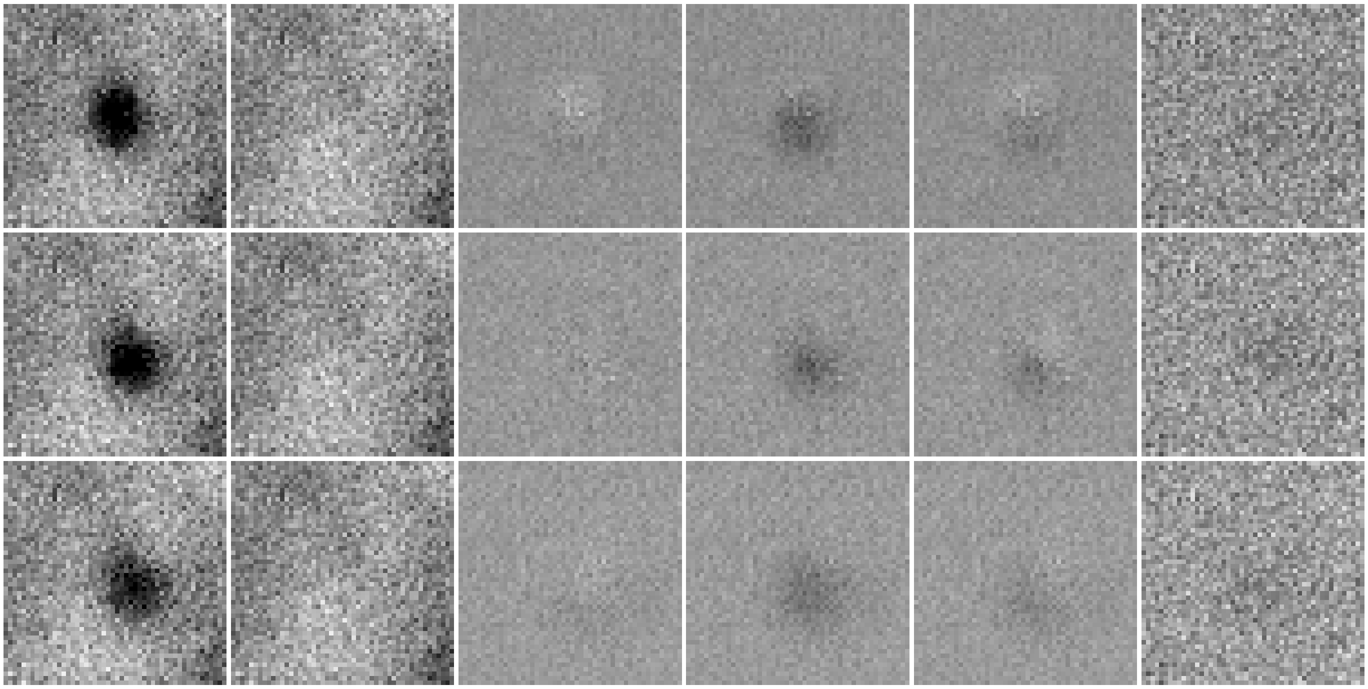

Fig. 17. Same as Figure 15 but for frame C in Figure 12 d.

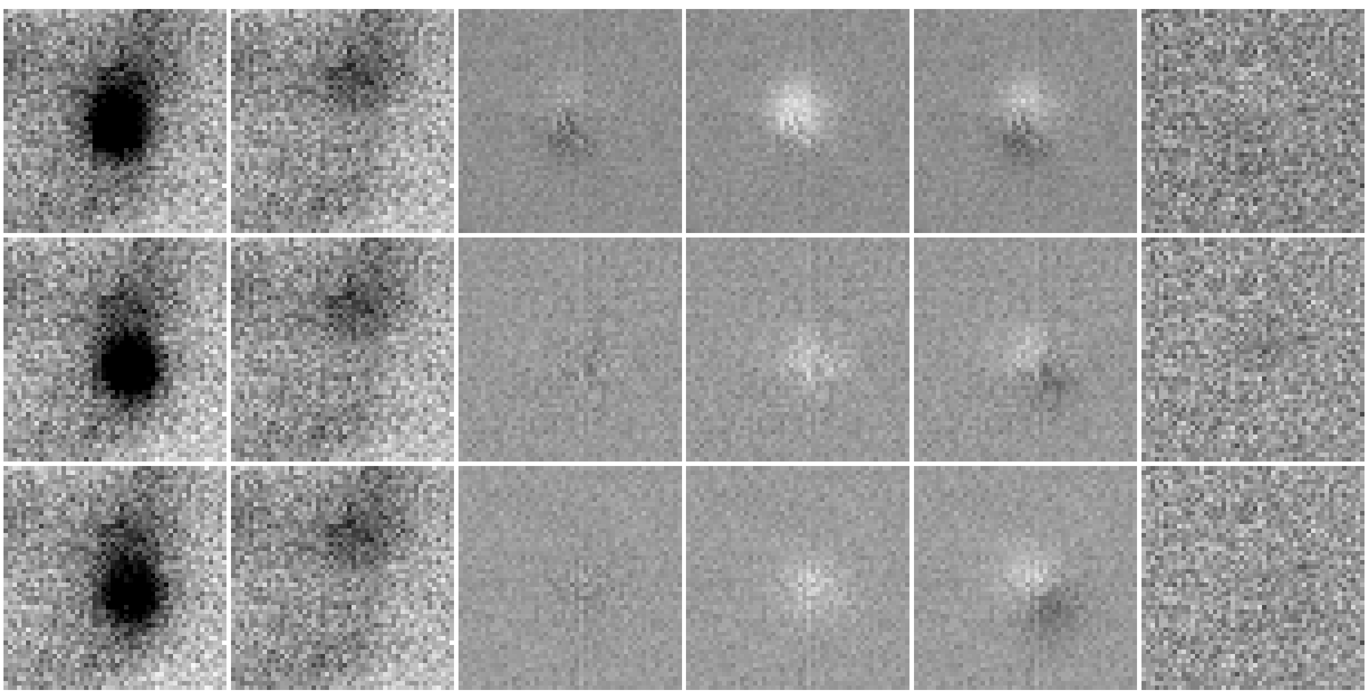

Fig. 18. Same as Figure 15 but for frame D in Figure 12 d.